Atmos. Chem. Phys. Discuss., 11, 11959–11993, 2011
www.atmos-chem-phys-discuss.net/11/11959/2011/
doi:10.5194/acpd-11-11959-2011

Atmospheric Chemistry and Physics Discussions

Snow optical properties at Dome C, Antarctica – implications for snow emissions and snow chemistry of reactive nitrogen

J. L. France[1], M. D. King[1], M. M. Frey[2], J. Erbland[3], G. Picard[3], A. MacArthur[4], and J. Savarino[3]

[1]Department of Earth Sciences, Royal Holloway University of London, Egham, Surrey, TW20 0EX, UK
[2]British Antarctic Survey, Highcross, Madingley Road, Cambridge CB3 0ET, UK
[3]UJF-Grenoble 1/CNRS-INSU, Laboratoire de Glaciologie et Géophysique de l'Environnement UMR 5183, St.-Martin-d'Hères, France
[4]NERC Field Spectroscopy Facility, Grant Institute, School of GeoSciences, University of Edinburgh, Edinburgh, EH9 3JW, UK

Received: 24 March 2011 – Accepted: 6 April 2011 – Published: 18 April 2011

Correspondence to: J. L. France (j.france@es.rhul.ac.uk)

Published by Copernicus Publications on behalf of the European Geosciences Union.

Abstract

Measurements of *e*-folding depth, nadir reflectivity and stratigraphy of the snowpack around Concordia station (Dome C, 75.10° S, 123.31° E) were undertaken and used to determine wavelength dependent coefficients (350 nm to 550 nm) for light scattering and absorption and to calculate potential fluxes of nitrogen dioxide (NO_2) from the snowpack due to nitrate photolysis within the snowpack. The stratigraphy of the top 80 cm of Dome C snowpack generally consists of three main layers: a surface of soft windpack (not ubiquitous), a hard windpack and a hoar-like layer beneath the windpack(s). The *e*-folding depths are ~10 cm for the two windpack layers and ~20 cm for the hoar-like layer for solar radiation at a wavelength of 400 nm, about a factor 2–4 larger than previous model estimates for South Pole. Depth integrated photochemical reaction rates of nitrate photolysis in the Dome C snowpack were calculated to give molecular fluxes of NO_2 of 5.3×10^{12} molecules m^{-2} s^{-1}, 2.3×10^{12} molecules m^{-2} s^{-1} and 8×10^{11} molecules m^{-2} s^{-1} for solar zenith angles of 60°, 70° and 80° respectively for clear sky conditions using the TUV-snow radiative-transfer model. Depending upon the snowpack stratigraphy, a minimum of 85% of the NO_2 originates from within the top 20 cm of the Dome C snowpack. It is found that on a multi-annual scale, nitrate photolysis can remove up to 80% of nitrate from surface snow, confirming independent isotopic evidence that photolysis is an important driver of nitrate loss occurring in the EAIS snowpack. However, the model cannot account for the total observed nitrate loss of 90–95% or the shape of the observed nitrate depth profile. A more complete model will need to include also physical processes such as evaporation, re-deposition or diffusion between the quasi-liquid layer on snow grains and firn air to account for the discrepancies.

ACPD

11, 11959–11993, 2011

1 Introduction

It is well documented that the photolysis of nitrate (NO_3^-) within snowpack is a source of NO_2 to the atmosphere above, with experiments in both North and South polar regions demonstrating that NO_x fluxes are emitted from the snowpack under sunlit conditions (e.g. Jones et al., 2001; Oncley et al., 2004; Honrath et al., 2002; Domine and Shepson, 2002). Snowpack photochemistry is reviewed in Grannas et al., (2007) and in the interest of brevity will not be further discussed. The reaction pathway for the emissions of NO_x is shown in Eqs. (1) and (2).

$$NO_3^- + h\nu \rightarrow NO_2 + O^- \quad \text{(R1a)}$$

$$NO_3^- + h\nu \rightarrow NO_2 + O(^3P) \quad \text{(R1b)}$$

$$NO_2^- + h\nu \rightarrow NO + O^- \quad \text{(R2)}$$

$$NO_2^- + OH \rightarrow NO_2 + OH^-$$

The reaction pathway (Reaction R1a) has been demonstrated in the laboratory to be 82–88 % more efficient than pathway (Reaction R1b) in both aqueous phase (Warneck and Wurzinger, 1988) and ice phase (Dubowski et al., 2001). The amount of NO_2 photochemically produced is dependent upon the concentration of nitrate within the snowpack, snowpack temperature and the intensity of solar radiation within the snowpack. The intensity of solar radiation penetrating into the snow is dependent upon the light scattering and absorption properties of the snowpack and the solar zenith angle. Snowpack can be split into two depth regimes based upon the propagation of solar radiation into the snow: a top layer, a few cm thick where direct solar radiation is converted into diffuse radiation, and a second layer, the asymptotic zone, below the top layer, in which, the solar radiation is effectively all diffuse and the intensity of the radiation decays exponentially (Warren, 1982).

ACPD
11, 11959–11993, 2011

The production of NO_2 within the snowpack provides a source of NO_x to the overlying atmosphere with large mixing ratios of NO (relative to remote regions) having been measured in boundary layer air at the South Pole and across the Antarctic plateau during several field campaigns (e.g. Davis et al., 2004; Davis et al., 2001; Davis et al., 2008; Oltmans et al., 2008). It is hypothesised that highly enhanced NO_x mixing ratios formed through the continued photochemical release of NO_x from the snowpack as air masses travel over the Antarctic plateau snow, cause the enhanced ozone concentrations measured over the South Pole (Neff et al., 2008; Legrand et al., 2009).

At locations with a low snow accumulation rate, such as Dome C on the Antarctic plateau (~7.2 cm yr^{-1}) (Rothlisberger et al., 2002; Wolff et al., 2002), nitrate deposited in the snow will spend a longer period of time nearer the surface than nitrate deposited in regions with higher snow accumulation rates such as Summit, Greenland (accumulation rate of 22 cm yr^{-1}) (Drinkwater et al., 2001). The availability of nitrate at the snow surface, or near to the snow surface, for long periods of time increases the probability that it will be photolysed and that photolysis products will be lost to the atmosphere before it is buried to sufficient depth to be preserved in ice-core records. Field and laboratory data suggest that on the Antarctic Plateau, nitrate photolysis is an important, possibly even the dominating process in driving nitrate out of the snow on the Antarctic plateau in the form of volatile nitrogen species (Frey et al., 2009b; Chu and Anastasio, 2003). A quantitative interpretation of the nitrate record from long ice core records such as the 800 kya old EPICA ice core recovered at Dome C is currently not possible since the understanding of post-depositional processes affecting nitrate is not complete (Jouzel et al., 2007; Wolff et al., 2010). An initial model study concluded that photochemistry can only account for 40% of the nitrate loss observed for the South Pole, with other post depositional processes being required to explain the depth profiles observed (Wolff et al., 2002). First isotopic evidence from laboratory photolysis experiments appeared to support this view (Blunier et al., 2005), however Frey et al. (2009a) showed that the laboratory results, and thus the conclusions drawn in Blunier et al. (2005) do not apply to the snow environment at the Earth's surface, including Dome C. To the

ACPD
11, 11959–11993, 2011

contrary, a model for photolytic isotopic fractionation explains within the analytical uncertainties the enrichment of the nitrogen stable isotope in snow nitrate observed at Dome C and in previous lab experiments, suggesting that photolysis is an important process driving fractionation and associated nitrate loss from snow, specifically in the low accumulation regions of EAIS (Frey et al., 2009b). However, more details on snow optical properties and how solar radiation propagates in snow are needed in order to further quantify processes contributing to post-depositional isotopic fractionation and change in snow chemistry. The latter is of high relevance for the interpretation of ice core records recovered at the site (e.g. Rothlisberger et al., 2000; Wolff et al., 2010).

In the work described here, the snowpack optical properties at Dome C from field measurements of snow surface reflectance and light penetration into the snowpack are determined. Using the field data with an 8-stream DISORT (Stamnes et al., 1988) radiative-transfer model, TUV-snow (Lee-Taylor and Madronich, 2002), the production of NO_2 within the Antarctic Plateau snowpack is calculated. Further, a comparison to the work of Wolff et al. (2002) and to NO_x flux measurements made during Antarctic Plateau field campaigns is undertaken, updating the modelling work undertaken in Wolff et al. (2002) using new field measurements obtained in this work. The resulting data updates estimations of NO_x emissions over the Antarctic plateau and provides evidence whether photochemistry alone can produce the NO_2 fluxes measured over the Antarctic plateau.

The aims of this work are to give:

1. A determination of the optical properties of Dome C snowpack to compare with measurements of other snowpack sites.

2. Calculation of fluxes of NO_2 from Dome C snowpack, and comparison with previously modelled and measured fluxes of NO_x from Antarctic snows.

ACPD
11, 11959–11993, 2011

2 Methods

The work was a field and modelling study of the Dome C snowpack, and each aspect (field and modelling) is described separately. The fieldwork characterises the optical properties of the Dome C snowpack that are required to calculate the fluxes of NO_2 due to snowpack photochemistry.

To estimate fluxes of NO_2 from the Dome C snowpack the coupled 8-stream snow-atmosphere radiative-transfer model TUV-snow was used (Lee-Taylor and Madronich, 2002). The TUV-snow model requires the snowpack to be optically parameterised in terms of scattering and absorption coefficients. To determine optical coefficients of absorption and scattering requires measurements of light penetration depth into the snow, snowpack reflectance and snow density.

2.1 Field methods

The snowpack light absorption and scattering were characterised by measurements of the nadir reflectivity and light penetration depth. Details of the methods can be found in Fisher et al. (2005).

Surveys of the snowpack at Dome C, with 12 snowpits at sites 1 km South, 5 km East and 1 km West of the Base, demonstrated that the top metre of snow cover consists of typically 3 distinct layers (with minor perturbations), and it is appropriate to consider the optical properties for each layer individually to allow the determination of optical coefficients for each layer.

2.1.1 *e*-folding depth measurements

From the measurements of in-snow irradiance at several levels within the snowpack, *e*-folding depths were calculated according to the Beer-Bouger Lambert law (Eq. 1), for each of the three layers.

$$I_z = I_{z'} e^{\frac{(z-z')}{\varepsilon(\lambda)}}, \quad (1)$$

ACPD
11, 11959–11993, 2011

Where I_z is the intensity at a depth z within the snowpack, z' is the initial depth into the snowpack, z is a deeper depth than z', and $\varepsilon(\lambda)$ is the wavelength (λ) dependent asymptotic e-folding depth (the depth at which incident diffuse irradiance has been reduced to $1/e$ (~37%) of its initial value) for a specific wavelength (λ).

The e-folding depth of the snowpack is calculated from measurements of the in-snow irradiance at different depths within the asymptotic zone. Further details can be found in Fisher et al. (2005)

The in-snow irradiance of the Dome C snowpack was measured within 14 separate snowpits at three areas in the vicinity of Dome C (within 5 km). For each snowpit, stratigraphy was recorded to gain an understanding of the natural variation in layer thickness but only the layers greater than 25 cm thick were selected for e-fold and albedo measurements.

Each snowpit was approximately 1.5 m by 1 m by 1 m and the irradiance penetrating into the snowpack was recorded using a custom built 6 spectrometer instrument with components from Ocean Optics. The method used here is a progression from the single fibre optic and single channel spectrometer method used during previous campaigns to measure snowpack optical properties (Beine et al., 2006; Fisher et al., 2005; King and Simpson, 2001). The spectrometers were powered through a single USB cable connected to a Panasonic toughbook computer allowing true field portability. Each spectrometer had its own fibre optic probe with a cosine corrector, which was placed horizontally into the fresh, shaded snowpack face, recorded UV-Visible radiation ($\lambda = 320 - 700$ nm, $\Delta\lambda \leq 1$ nm) within the snowpack at varying depths in a single stratigraphic layer. The signal to noise ratio was typically better than 1:500. The vertical spacing between each fibre was approximately 3–5 cm where the thickness of the snowpack layer allowed, and no fibres were placed within 3 cm of a snow layer boundary. Optical measurements of thick layers ensures the variation of solar irradiance within the snow layer was measured over 2 or more times the e-folding depths in each layer and is indeed characteristic of that layer. The fibres were displaced horizontally by 10–30 cm. A relative intensity calibration of the spectrometers and fibre optics was

ACPD
11, 11959–11993, 2011

performed by simultaneously measuring the intensity of the solar radiation above the snowpack. Dark spectra (electrical noise) were also recorded in the field by capping the fibre optic probes. A wavelength calibration for each spectrometer was performed using a mercury-argon lamp in the field. The 6 spectrometer instrument recording at different depths simultaneously means no correction for changing sky conditions is required. The *e*-folding depth does not depend upon the absolute irradiance, measured by each spectrometer, and therefore there is no need for an absolute irradiance calibration of the fibre optic probes or spectrometer efficiency, although a travelling NIST illumination standard was used to monitor equipment for quality assurance purposes and long term drift.

2.1.2 Nadir reflectance

Measurements of surface nadir reflectance (reflectivity) were carried out using a Dual Field of View (DFoV) nadir reflectance method (Duggin and Philipson, 1982). Two GER1500 spectroradiometers were placed on tripods viewing vertically downwards, with one measuring upwelling radiance from the snow surface and the second spectroradiometer simultaneously measuring the upwelling radiance from a white spectralon plate of known and carefully calibrated reflectance. Using simultaneous measurements of both the measured snowpack and the reference minimises any effect of changing overhead sky conditions. The two GER1500 spectroradiometers were cross-calibrated in the field by simultaneously measuring the reflectance of the spectralon plate multiple times. Using a 3° fore optic, the viewing footprint of the spectroradiometers measured 8 cm diameter on the measured surface. The spectroradiometers and spectralon plate are maintained and calibrated by the UK NERC Field Spectroscopy Facility.

The technique to determine scattering and absorption coefficients requires a measurement of the reflectivity and the *e*-folding depth of each layer. For the non-outcropping layers the overlying snowpack was carefully removed with a clean aluminium shovel. An area approximately 3×3 m was cleared.

ACPD
11, 11959–11993, 2011

Measurements were also made of snowpack density with depth (using a 200 cm^3 cutting box, similar to a version tested in Conger and McClung, 2009), basic snowpack stratigraphy (Fierz et al., 2009) and for the purpose of photochemical calculation, a snowpack temperature depth profile.

2.2 Modelling snowpack optical coefficients of scattering and absorption

Using the TUV-snow radiative-transfer model (Lee-Taylor and Madronich, 2002) a wavelength dependent absorption cross-section due to light-absorbing impurities in the snow, σ^{+}_{abs}, and scattering cross-section, $\sigma_{scatt,}$ were determined from the field measurements of *e*-folding depth, reflectivity and snowpack density for each layer. The TUV-snow radiative-transfer model has been used successfully to parameterise snowpack optical coefficients, σ^{+}_{abs} and σ_{scatt}, from field measurements made on several previous cold region campaigns (Beine et al., 2006; Fisher et al., 2005; France et al., 2010; King et al., 2005; Lee-Taylor and Madronich, 2002), and has been validated using chemical actinometry with laboratory snow (Phillips and Simpson, 2005). A detailed description of the procedure to determine the scattering and absorption coefficients from *e*-folding depth and nadir reflectance is given by Lee-Taylor and Madronich (2002), but a brief summary is given here.

Irradiances in snow are modelled using a range of values of σ_{scatt} and σ^{+}_{abs} and values of asymptotic *e*-folding depth and surface reflectance are calculated. The values of σ_{scatt} and σ^{+}_{abs} are tuned until a unique match between the field measured *e*-fold and reflectance and modelled *e*-fold and reflectance is found. The TUV-snow model (Lee-Taylor and Madronich, 2002) is a DISORT (Stamnes et al., 1988) coupled atmosphere-snow model running 8 streams with a pseudo-spherical correction. There are 80 atmospheric levels with 1 km spacing, 106 snowpack levels (with 1 mm spacing in the top 0.5 cm and 1 cm spacing for the rest of the 1 m of snowpack), clear sky conditions, no overhead aerosol, an earth-sun distance based upon 1 January 2010, under snow albedo of 0.95, an asymmetry factor of 0.89 for the 100 µm snow grains, and an

ACPD
11, 11959–11993, 2011

overhead column ozone of 300 Dobson Units (Ozone determined from measurements by the Ozone Monitoring Instrument, values during the season range from 260–340 DU, (McPeters et al., 1998)). Using TUV-snow to determine the effect of ozone column variation on nitrate photochemistry, an increase in ozone from 260 to 340 DU results in a 14% decrease in surface nitrate photochemistry.

The method outlined produces a unique solution for σ_{scatt} and σ^{+}_{abs} that satisfy both the measured reflectivity and *e*-folding depth for a specified wavelength. Values of σ_{scatt} and σ^{+}_{abs} are determined for wavelengths 350–550 nm at 25 nm intervals.

2.3 Snowpack chemical measurements

Measurements of depth resolved nitrate concentrations in snow at the Dome C station were co-located with the main area of snowpack *e*-folding depth measurements (75.1047° S 123.3390° E). A 30 cm snow pit was sampled using 50 ml Greiner PP centrifuge tubes that were previously rinsed with MilliQ quality water. Snow was collected every centimetre for the top 20 cm of the snowpack and one additional sample was taken at 30 cm deep. Nitrate concentrations were determined by a colorimetric method using a continuous flow analysis system in the field (Frey et al., 2009b). The precision of this method is better than 3% in the range 10 to 1000 ng g^{-1}.

2.4 Modelling in-snow nitrate photochemistry

Nitrate photolysis rate coefficients, $J_{NO_3^-}(\theta, z)$ are calculated as shown in Eq. (2).

$$J_{NO_3^-} = \int_{\lambda_1}^{\lambda_2} \sigma(\lambda, T)\Phi(\lambda, T)I(\lambda, \theta, z)d\lambda \quad (2)$$

Where σ is the absorption cross-section, λ is the wavelength, T is the temperature, z is the depth into the snowpack, I is the spherical irradiance (actinic flux) within the snowpack, θ is the solar zenith angle and Φ is the quantum yield.

ACPD
11, 11959–11993, 2011

The temperature-dependant quantum yield of Reaction (R1) on ice and the absorption cross-section of nitrate in aqueous solution are both taken from Chu and Anastasio (2003). Other available quantum yield data for 308 nm photolysis of nitric acid on ice films of 0.92±0.26 (Zhu et al., 2010) seem extremely high compared with previous data (Chu and Anastasio, 2003; Warneck and Wurzinger, 1988; Zellner et al., 1990), but if correct would increase the NO_2 production by a factor of ~400.

Photolysis rate coefficients are calculated at 126 depths (with extra 1 mm layers 0.5 cm each side of snow layer boundaries added when compared with spacing used to determine absorption and scattering coefficients within single layers) within a 1 m semi-infinite model snowpack, using the optical coefficients determined for a wavelength of 350 nm, snowpack layer thicknesses, densities and snow temperatures as described in Table 1. Values in Table 1 are from the results of this paper, however, reference is made to these values now for overall clarity of the methods used. The 350 nm values of σ_{scatt} and σ^{+}_{abs} are used for the calculation of the photochemical rate coefficients as the maximum in the action spectrum of nitrate photolysis is ~320 nm (Chu and Anastasio, 2003).

A molecular flux of NO_2 from the snowpack, $F(NO_2)$, as a function of solar zenith angle, is calculated from $J_{NO_3^-}(\theta,z)$ as shown in Eq. (3), and the value of J for Eq. (2) is calculated as a function of solar zenith angle and depth.

$$F(NO_2) = \int_{z=0\,m}^{z=1\,m} \left[NO_3^-\right]_z J(\theta,z)dz \quad (3)$$

where z is the depth into the snowpack, $\left[NO_3^-\right]$ is the concentration of nitrate in moles per unit volume, $J(\theta,z)$ is the photolysis rate constant as a function of solar zenith angle and depth.

The flux of NO_2 assumes 100% of NO_2 produced by photolysis escapes the snowpack and does not undergo any gas phase chemistry

ACPD
11, 11959–11993, 2011

3 Results

The results are presented in three sections the field data, determination of optical coefficients from the Dome C snowpack and the calculation of fluxes of NO_2 due to in-snow nitrate photochemistry.

3.1 Field results

The measurements of snowpack stratigraphy, temperature and density are shown in Fig. 1. The description of the stratigraphy is generalised from 14 snowpits dug around the Dome C base with comparable snowpack stratigraphy seen in each snowpit, four examples of real snowpack stratigraphy measurements are shown in Fig. 1. The 2010 stratigraphy is comparable with other previously reported stratigraphy for Dome C (Fierz et al., 2009; Gallet et al., 2011; Warren et al., 2006). The stratigraphy at Dome C is two windpack layers overlaying a hoar layer, thought to be formed through temperature gradient snow metamorphism (Gallet et al., 2011). The temperature profile with depth shows in Fig. 1 that snowpack temperature decreases ~10 °C with 60 cm of snow depth. Snowpack nitrate concentration profiles for Dome C snowpits measured during the campaign are shown in Fig. 2.

The median *e*-folding depths calculated for the three snowpack layers are shown in Fig. 1, along with the corresponding nadir reflectivity measurements for the same snowpacks. The median value of the *e*-folding data is used so that a matching albedo measurement is used to model each snow layer, rather than a composite measurement from several sites. The maximum *e*-folding depth occurs around 390 nm in the hoar layer, whereas the maximum *e*-folding in the windpacked layers is around a wavelength of 420 nm. The reflectivity data shows that the maximum reflectance occurs between 450 nm and 500 nm for each of the snowpack layers. A similar pattern of reflectance and light attenuation maxima is also considered in Warren (2006) and explained through the presence of snowpack impurities with wavelength dependent absorptions.

ACPD
11, 11959–11993, 2011

3.2 Snowpack optical coefficients

Values of the optical coefficients (σ_{scatt} and σ^{+}_{abs}) are reported for wavelengths of 350 nm (Table 1) and 400 nm (Table 2). Data in Table 1 is used for the calculation of $JNO_3^-(\theta,z)$ and data in Table 2 is to allow comparison of Dome C snowpack optical coefficients to other snowpack measurements.

The absorption of light in the snowpack is due to absorption by water ice (weak absorption in the visible) and impurities in the snowpack. Plotting σ^{+}_{abs} vs. λ in Fig. 3 demonstrates the absorption in the snowpack owing to impurities. It is thought that absorption is dominated by the presence of black carbon (Lee-Taylor and Madronich, 2002). The variation of σ^{+}_{abs} with wavelength, as shown in Fig. 3, decreases with increasing wavelength and matches well to a scaled measurement of the absorption spectrum of HULIS (Hoffer et al., 2006). The implication is that the impurities at Dome C are due to atmospheric deposition of HULIS, and black carbon, rather than primarily black carbon. The absorption due to black carbon would be relatively invariant with wavelength across the UV-visible wavelength range. If the maximum contribution of black carbon is assumed to be the absorption at the lowest point of our derived absorption cross-section, (similar method is applied in Doherty et al., 2010), then the amount of black carbon in the snow at Dome C varies between 2 and 6 ng g^{-1}, similar to the 3.3 ppb measured in the surface snow in 2004 at Dome C by Warren et al., (2006). The value of σ_{scatt} is generally invariant with wavelength (typically ±10% per 100 nm).

To determine the magnitude of uncertainty in the estimates of black carbon concentrations, the ±2 standard deviations of uncertainty in albedo (the largest source of uncertainty in the field measurements) were propagated through into the determination of wavelength dependent absorption coefficients. The resulting maximum black carbon concentration, accounting for uncertainty in the snowpack albedo, varies between ~0 ng g^{-1} and 13 ng g^{-1}.

ACPD
11, 11959–11993, 2011

3.3 Dome C in-snow nitrate photolysis rate coefficients

The photolysis rate coefficients for Reaction (R1a) calculated at each of the 126 depths within the snowpack for nitrate photolysis are shown as contours of equal $J\mathrm{NO}_3^-$ versus depth and solar zenith angle in Fig. 4. Figure 4 highlights two main points: the variation of $J\mathrm{NO}_3^-$ with solar zenith angle and depth between the two windpacked layers is very small, thus validating previous studies where previous Antarctic windpacked snows were treated as a bulk despite small changes in stratigraphy (Beine et al., 2006) and secondly, that the change in variation of $J\mathrm{NO}_3^-$ with solar zenith angle and depth for the hoar-like layer is extremely pronounced and shows that the use of a multi-layer snowpack model should be considered where optical properties are very different between layers.

3.4 NO_2 fluxes

The potential flux of NO_2 (disregarding cage effects, diffusion, conversion prior to emission and forced ventilation from the snowpack) from the snowpack owing to nitrate photolysis within the snowpack versus solar zenith angle, calculated using the nitrate profile shown in Fig. 2 and Eq. (3), is shown in Fig. 5. Figure 5 is calculated for clear sky conditions and assumes all photoproduced NO_2 is released from the snowpack. Figure 5 allows a simple comparison with previous measurements of NO_x fluxes at Antarctic sites.

4 Discussion

The discussion is split into 4 sections:

1. A comparison of field measurements with other snowpack environments and previous measurements at Dome C and analysis of the variation of the optical coefficients with wavelength.

ACPD
11, 11959–11993, 2011

2. A discussion of the optical coefficients (σ_{scatt} and σ^{+}_{abs}), with comparison to previously determined values of σ_{scatt} and σ^{+}_{abs}, and a discussion of variation between snowpack layers at Dome C.

3. An overview of the calculated rates of $J_{NO_3^-}(\theta,z)$ within the snowpack and the fluxes of NO_2.

4. A comparison with the modelled values of $F(NO_2)$ for the Antarctic Plateau with the work of Wolff et al. (2002) and the impact of photochemistry on the preservation of nitrate with depth into the snowpack.

4.1 Comparison of field measurements

The stratigraphy of Dome C snowpack is relatively constant within the vicinity of the base (<5 km), with thicknesses of the snowpack layers varying from 0 cm to 35 cm for the soft windpack (Layer A) and 5 cm to 65 cm for the hard windpack (Layer B). The hoar-like layer (Layer C) was ubiquitous at Dome C below the windpack and was at least 50 cm thick at each site visited. Minor layers such as 1 mm thick icy layers were noted in the detailed stratigraphy as shown in Fig. 1, but were not present at every site and were too thin to determine an *e*-folding depth using the fibre optic probe method. Given the consistency of *e*-fold measurements within layers, it appears that the thin icy layers do not have a measurable effect. Figure 4 also demonstrates that the calculation of $J\mathrm{NO}_3^-$ is not sensitive to the relative amounts of soft or hard windpack, the major change in $J\mathrm{NO}_3^-$ occurs with the transition from windpack to the hoar-like layer.

The *e*-folding depths show there are two main optical layers, a windpack layer, either soft or hard, which have asymptotic *e*-folding depths of ∼10 cm at a wavelength of 400 nm and a depth-hoar-like layer which has an asymptotic *e*-folding depth of ∼20 cm at a wavelength of 400 nm. The combined thickness of the windpack layers is typically 20–35 cm. As previously determined, 85% of the photochemistry occurring in snowpack occurs in the top 2 *e*-folding depths (King and Simpson, 2001), so at Dome C, at

ACPD
11, 11959–11993, 2011

least 85% of the photochemistry occurs in the windpacked layers. However, it is worth noting that up to 15% of the photochemistry could be occurring in the hoar-like layer. The process of photochemistry occurring in hoar-like layers (to our knowledge) has not been investigated. The measured *e*-folding depths are longer than the 3.7 cm at 320 nm previously calculated by Wolff et al. (2002) by a factor of ∼3. Layer C is similar to the *e*-folding depth values measured in snowpack at depths between 40 and 90 cm of ∼20 cm for wavelengths between 380 nm and 450 nm, as investigated in Warren et al., (2006). The *e*-folding depth of ∼3 m at 380 nm for a snow depth of 90 – 135 cm measured in Warren et al., (2006) is far larger than any measurements of e-folding depth made in the top 50 cm of snowpack during this work. However, these deeper, highly transmittive snowpack layers as measured by Warren et al., (2006) do not have a significant influence upon the photochemistry occurring in the snowpack as they are too deep within the snow.

Microwave emissivity data determining average snow grain size in the top ∼20 cm of snowpack across Antarctica show that around Dome C and the majority of the East Antarctic plateau average grain size is 0.5 to 0.6 cm (Brucker et al., 2010). The average grain size determined for the top 20 cm of snow at Dome C from field measurements is consistent with the microwave emissivity data (Table 1), suggesting that the snowpack at Dome C is not unrepresentative of the typical East Antarctic plateau snowpack.

4.2 Optical coefficients of Dome C snowpack

The absorption cross-sections for the three snowpack layers in Fig. 3 show an increased absorption in the UV region compared to minimum absorption occurring at a wavelength around 500 nm. The absorption is mainly due to snowpack impurities (Warren et al., 2006). A black carbon impurity would absorb almost uniformly across the wavelength range 350–550 nm. Absorption with increasing wavelength indicates the presence of UV absorbing compounds in the snowpack such as humic material or HULIS (HUmic LIke Substances), albeit in very small concentrations. Previous measurements of black carbon in the Dome C surface snowpack made in 2004 measured

ACPD
11, 11959–11993, 2011

3.3 ng g^{-1} of black carbon and 26 ng g^{-1} of dust (Warren et al., 2006). The amount of absorption due to impurities determined through the measurements of light transmission and albedo in this work can be described as black carbon equivalent by approximating 10 ng g^{-1} of black carbon equivalent to 1 cm^2 kg^{-1} (Lee-Taylor and Madronich, 2002). The range of maximum black carbon concentration in the Dome C snowpack measured in this work of 2–6 ng g^{-1} is comparable to the 3.3 ng g^{-1} of black carbon measured by Warren et al., (2006) in the surface snow. However, absorption in the UV and blue wavelength ranges in all three snowpack layers is increased. This is likely due to the presence of small quantities of an unknown UV-visible absorber, with preferential absorption in the UV and small amounts of black carbon as a composite absorption due to HULIS and black carbon as comparison with our measurements of the respective absorption cross sections shows (Fig. 3). HULIS has been widely seen in Arctic snowpack and seems the most likely explanation to the absorption patterns seen in Fig. 3. The increased absorption in the UV cannot be attributed to nitrate, as the increase in absorption begins at wavelengths longer than 340 nm.

The optical coefficients, σ_{scatt} and σ^{+}_{abs}, at Dome C are compared to previously determined values for other snowpacks in Table 2. The optical coefficients are taken for a wavelength of 400 nm to provide direct comparisons with previous literature. The absorption cross-section at a wavelength of 400 nm is small compared to other sites globally, although slightly larger than other Antarctic locations (Lee-Taylor and Madronich, 2002). It has been noted that in very clean snowpack locations, as in Antarctica, the albedo is close to unity and the estimates of absorption and scattering co-efficients are very sensitive to the albedo (Lee-Taylor and Madronich, 2002).

4.3 NO_2 fluxes from the Dome C snowpack

The potential molecular flux of gaseous NO_2 from the snowpack can be compared to fluxes of NO_x estimated from measured NO fluxes from Antarctic plateau snow to give fluxes of $\sim 4 \times 10^{12}$ molecules m^{-2} s^{-1} (24 nmol m^{-2} h^{-1}) for a solar zenith angle around

ACPD
11, 11959–11993, 2011

68° (Oncley et al., 2004). Modelled NO_x flux data from the same campaign determined an average of 3.2–4.2×10^{12} molecules m^{-2} s^{-1} (19–25 nmol m^{-2} h^{-1}) (Wang et al., 2007). Coastal Antarctic fluxes of NO_x from the snowpack were measured during early February, 2005 with mean daily fluxes of 1.7–3.4×10^{12} molecules m^{-2} s^{-1} (10–20 nmol m^{-2} h^{-1}) (Bauguitte et al., 2009).

For Dome C, a flux of NO_2 of 2.4–3.8×10^{12} molecules m^{-2} s^{-1} (14–23 nmol m^{-2} h^{-1}) is predicted for a solar zenith angle of 68° (Fig. 5) similar in magnitude to the NO_x flux estimated during the ISCAT campaign at South Pole.

4.4 Comparison with previous Antarctic plateau nitrate photolysis modelling

Photolysis of nitrate in polar snow removes nitrate from the snowpack and provides a source of NO_2 to the overlying atmosphere, resulting in lower concentrations of nitrate with depth into the snowpack (as seen in Fig. 2). Previous work estimating fluxes of NO_2 and modelling nitrate loss with depth within the snowpack for a theoretical Antarctic snowpack (located at the South Pole) predicted a maximum NO_2 flux of 1.4×10^{12} molecules m^{-2} s^{-1} (8 nmol m^{-2} h^{-1}) from the snowpack and that a maximum of 40% of the nitrate loss can be attributed to the photochemical depletion of nitrate within the snow (Wolff et al., 2002). However, the work of Wolff et al. (2002) assumed an *e*-folding depth of 3.7 cm and a snowpack stratigraphy uniform with depth. The following updates between this work and Wolff et al. (2002) were made: the absorption cross-section (measured in aqueous solution at 278 °K) and the quantum yield (measured on ice pellets) for nitrate photolysis is from Chu and Anastasio (2003) rather than Burley and Johnston (1992), and the ice absorption spectrum is taken from Warren (2008). The model snowpack is input in the 8-stream TUV-snow model (Lee-Taylor and Madronich, 2002) (vs. the 4-stream radiative-transfer model used in Wolff et al., 2002) using the measured optical coefficients (Table 1), rather than an assumed e-folding depth of 3.7 cm as used in the model of Wolff et al. (2002). The radiative-transfer model used in Wolff et al. (2002) was an in-house British Antarctic Survey

ACPD
11, 11959–11993, 2011

model (Gardiner and Martin, 1997). For the calculation of NO_2 fluxes from the snowpack, the nitrate concentration of 100 µmol kg^{-1} in the surface snow chosen in Wolff et al. (2002) is replaced with the nitrate profiles in Fig. 2. A maximum, minimum and median NO_2 flux is shown from using the nitrate profiles in Fig. 2.

The comparison between the calculations of snowpack NO_2 production rates of Wolff et al. (2002) and this work is shown in Fig. 6. Figure 6 shows that with the updated radiative-transfer modelling for a Dome C type snowpack at a South Pole location gave a 3-fold increase in the NO_2 production from Antarctic snowpack for the same solar zenith angles when compared to Wolff et al. (2002); a combined effect of the longer *e*-folding depth than predicted in Wolff et al. (2002) and using a measured in snow nitrate profile. The increase in *e*-folding depth between the measured *e*-folding depth of this work and Wolff et al. (2002) is approximately a factor of 3.

The second part of the work reported in Wolff et al. (2002) demonstrated that the maximum loss of nitrate in the snow due to photochemistry is only 40%, with other processes such as re-evaporation invoked to explain the measured nitrate profiles such as seen in Fig. 2. In order to test whether this is the case with new *e*-folding data and stratigraphy measurements, data from Fig. 3 (Wolff et al., 2002) is reproduced using the nitrate photolysis rate constants calculated in this work. The calculated photolysis rate constants for nitrate photolysis versus depth and solar zenith angle shown in Fig. 4 were used to run a simple nitrate depletion model for South Pole and Dome C solar zenith angles. The initial snowpack nitrate concentration was assumed to be 100 µg kg^{-1} and a constant year round snow burial rate of 72 mm yr^{-1}. The model snowpack was split into levels 1 µm thick and the amount of photolysed nitrate calculated in each layer on a daily basis. After each day in the model, the snowpack was buried by 197 µm and fresh snow 197 µm deep containing 100 µg kg^{-1} of nitrate is deposited on the surface. This process was repeated for 10 years of daily solar zenith angles for both a South Pole locality and a Dome C locality. The modelled depth profile of nitrate, due to only photochemical loss, for a snowpit at a notional South Polar site and a Dome C site, calculated on a daily basis, is shown in Fig. 7, and is

ACPD
11, 11959–11993, 2011

compared directly with the work of Wolff et al. (2002). The modelled photochemical loss is also compared to a measured nitrate concentration profile at Dome C, (scaled to 100 µg kg^{-1} at the surface) to determine if photochemical depletion can reproduce a typical measured nitrate profile at Dome C. The bumps in the modelled signals are not always preserved in measured profiles, (Fig. 2) but other post depositional loss such as diffusion and re-evaporation processes would be expected to smoothen the profile (Wagenbach et al., 1994).

For South Pole solar zenith angles, the nitrate concentration in the snowpack can only be reduced by ∼60% of the initial concentration. For solar zenith angles at Dome C, the nitrate concentration can be reduced by ∼80% of the surface concentration. The rapidity of the nitrate loss at Dome C in the upper most part of the snowpack cannot be reproduced with a simplistic photochemical depletion model. The differences between modelled and measured nitrate profiles for Dome C and and South Pole depletion are due to the extended daylight period at Dome C compared to South Pole. The differences could be due to a number of effects, the re-deposition of nitrate at the surface, enhancing the surface concentrations relative to at depth, the continued evaporation of nitrate from within the snowpack, or an increased photolytic reaction rate of nitrate within the snowpack compared to laboratory measured values of the quantum yield (Zhu et al., 2010).

5 Conclusions

At Dome C, 85 % of the NO_x production from the photolysis of nitrate occurs in the top 20 cm of snow cover, with the majority of the remaining 15% of the snowpack photochemistry occurring in hoar-like layers. The *e*-folding depth in the windpacked snow layers is ∼10 cm at a wavelength of 400 nm and ∼20 cm at a wavelength of 400 nm in the hoar-like snow layer beneath the windpacks.

The composite absorption spectrum of impurities in the Dome C snowpack as shown by σ^{+}_{abs} vs λ is consistent with a λ dependent absorber, such as HULIS and

ACPD
11, 11959–11993, 2011

a wavelength independent black carbon absorption. The maximum black carbon concentration in Dome C snowpack is estimated at 2–6 ng g^{-1}.

The calculated flux of NO_2 from nitrate photochemistry in the snowpack on the Antarctic plateau at Dome C is of similar magnitude to fluxes of NO_x measured and modelled for a previous Antarctic campaign at the South Pole for equivalent solar zenith angles, with fluxes of NO_2 of 5.3×10^{12} molecules m^{-2} s^{-1}, 2.3×10^{12} molecules m^{-2} s^{-1} and 8×10^{11} molecules m^{-2} s^{-1} (32 nmol m^{-2} h^{-1}, 14 nmol m^{-2} h^{-1} and 5 nmol m^{-2} h^{-1}) calculated for solar zenith angles of 60°, 70° and 80° respectively for clear sky conditions at Dome C. Using the *e*-folding depths measured at Dome C, photochemistry of nitrate can only account for a maximum of ~60% of the depletion of nitrate concentration with depth in the snowpack at a notional South Polar site and ~80% of the depletion of nitrate at Dome C. Constraining the amount of nitrate depletion in snowpack at important ice-core drilling sites, such as Dome C, is an important step in beginning to understand the causes of isotopic shifts seen in nitrate records in snow and ice cores (Rothlisberger et al., 2000; Frey et al., 2009b).

Although a simple photochemical model cannot exactly re-produce nitrate concentration profiles seen in the snowpack as other factors such as re-evaporation must also play a role, it is evident that the photolysis of nitrate is the dominant process of nitrate loss in snowpack confirming recent isotopic evidence (Frey et al., 2009b).

Acknowledgements. We would like to thank Institut Polaire Paul-Emile Victor (IPEV) for logistical support in the field and staff at Dome C for all the support and help with this project, this study was partly funded by the program IPEV 1011 NITEDC. JLF and MDK thank NERC for support through grants NE/F0004796/1 and NE/F010788. This study benefited from support by project ANR 07 Vuln 013 "Vanish" and INSU-LEFE. MDK and JLF thank NERC FSF for support and expertise through grants 555.0608 and 584.0609 and Royal Holloway Earth Sciences research strategy fund awards.

ACPD
11, 11959–11993, 2011

References

Bauguitte, S. J. B., Bloss, W. J., Evans, M. J., Salmon, R. A., Anderson, P. S., Jones, A. E., Lee, J. D., Saiz-Lopez, A., Roscoe, H. K., Wolff, E. W., and Plane, J. M. C.: Summertime NOx measurements during the CHABLIS campaign: can source and sink estimates unravel observed diurnal cycles?, Atmos. Chem. Phys. Discuss., 9, 20371–20406, 10, http://www.atmos-chem-phys-discuss.net/9/20371/10/.5194/acpd-9-20371-2009, 2009.

Beine, H. J., Amoroso, A., Domin, F., King, M. D., Nardino, M., Ianniello, A., and France, J. L.: Surprisingly small HONO emissions from snow surfaces at Browning Pass, Antarctica, Atmos. Chem. Phys., 6, 2569–2580, doi:10.5194/acp-6-2569-2006, 2006.

Blunier, T., Floch, G. L., Jacobi, H. W., and Quansah, E.: Isotopic view on nitrate loss in Antarctic surface snow, Geophys. Res. Lett., 32, doi:10.1029/2005GL023011, L13501, 2005.

Brucker, L., Picard, G., and Fily, M.: Snow grain-size profiles deduced from microwave snow emissivities in Antarctica, J. Glaciol., 56, 514–526, 2010.

Burley, J. D. and Johnston, H. S.: Ionic Mechanisms for Heterogeneous Stratospheric Reactions and Ultraviolet Photoabsorption Cross-Sections for NO_2^+, HNO_3, and NO_3^- in Sulfuric-Acid, Geophys. Res. Lett., 19, 1359–1362, 1992.

Chu, L. and Anastasio, C.: Quantum yields of hydroxyl radical and nitrogen dioxide from the photolysis of nitrate on ice, J. Phys. Chem. A, 107, 9594–9602, 2003.

Conger, S. M. and McClung, D. M.: Comparison of density cutters for snow profile observations, J. Glaciol., 55, 163–169, 2009.

Davis, D., Nowak, J. B., Chen, G., Buhr, M., Arimoto, R., Hogan, A., Eisele, F., Mauldin, L., Tanner, D., Shetter, R., Lefer, B., and McMurry, P.: Unexpected high levels of NO observed at South Pole, Geophys. Res. Lett., 28, 3625–3628, 2001.

Davis, D., Chen, G., Buhr, M., Crawford, J., Lenschow, D., Lefer, B., Shetter, R., Eisele, F., Mauldin, L., and Hogan, A.: South Pole NO_x Chemistry: an assessment of factors controlling variability and absolute levels, Atmos. Environ., 38, 5375–5388, 2004.

Davis, D. D., Seelig, J., Huey, G., Crawford, J., Chen, G., Wang, Y. H., Buhr, M., Helmig, D., Neff, W., Blake, D., Arimoto, R., and Eisele, F.: A reassessment of Antarctic plateau reactive nitrogen based on ANTO 2003 airborne and ground based measurements, Atmos. Environ., 42, 2831–2848, doi:10.1016/j.atmosenv.2007.07.039, 2008.

Doherty, S. J., Warren, S. G., Grenfell, T. C., Clarke, A. D., and Brandt, R. E.: Light-absorbing impurities in Arctic snow, Atmos. Chem. Phys., 10, 11647–11680, doi:10.5194/acp-10-

ACPD
11, 11959–11993, 2011

11647-2010, 2010.
Domine, F. and Shepson, P. B.: Air-snow interactions and atmospheric chemistry, Science, 297, 1506–1510, 2002.
Drinkwater, M. R., Long, D. G., and Bingham, A. W.: Greenland snow accumulation estimates from satellite radar scatterometer data, J. Geophys. Res.-Atmos., 106, 33935–33950, 2001.
Dubowski, Y., Colussi, A. J., and Hoffmann, M. R.: Nitrogen dioxide release in the 302 nm band photolysis of spray-frozen aqueous nitrate solutions. Atmospheric implications, J. Phys. Chem. A, 105, 4928–4932, 2001.
Duggin, M. J. and Philipson, W. R.: Field measurement of reflectance: some major considerations, Appl. Opt., 21, 2833–2840, 1982.
Fierz, C., Armstrong, R. L., Durand, Y., Etchevers, P., Greene, E., McClung, D. M., Nishimura, K., Satyawali, P. K. and Sokratov, S. A.: The International Classification for Seasonal Snow on the Ground, IHP-VII Technical Documents in Hydrology No. 83, IACS Contribution No. 1, UNESCO-IHP, Paris, 2009.
Fisher, F. N., King, M. D., and Lee-Taylor, J.: Extinction of UV-visible radiation in wet midlatitude (maritime) snow: Implications for increased NOx emission, J. Geophys. Res., 110, D21301, doi:10.1029/2005JD005963, 2005.
France, J. L., King, M. D., and Lee-Taylor, J.: The importance of considering depth-resolved photochemistry in snow: a radiative-transfer study of NO_2 and OH production in Ny-Alesund snowpacks, J. Glaciol., 56(198), 655–663, 2010.
Frey, M. M., Hutterli, M. A., Chen, G., Sjostedt, S. J., Burkhart, J. F., Friel, D. K., and Bales, R. C.: Contrasting atmospheric boundary layer chemistry of methylhydroperoxide (CH3OOH) and hydrogen peroxide (H_2O_2) above polar snow, Atmos. Chem. Phys., 9, 3261–3276, doi:10.5194/acp-9-3261-2009, 2009a.
Frey, M. M., Savarino, J., Morin, S., Erbland, J., and Martins, J. M. F.: Photolysis imprint in the nitrate stable isotope signal in snow and atmosphere of East Antarctica and implications for reactive nitrogen cycling, Atmos. Chem. Phys., 9, 8681–8696, doi:10.5194/acp-9-8681-2009, 2009b.
Gallet, J.-C., Domine, F., Arnaud, L., Picard, G., and Savarino, J.: Vertical profiles of the specific surface area of the snow at Dome C, Antarctica, The Cryosphere Discuss., 4, 1647–1708, doi:10.5194/tcd-4-1647-2010, 2010.
Gardiner, B. G., and Martin, T. J.: On measuring and modelling ultraviolet spectral irradiance, in: Current problems in atmospheric radiation, edited by: Smith, W. L., and Stamnes, K.,

ACPD
11, 11959–11993, 2011

Deepak Hampton, Virginia, pp. 917–920, 1997.
Grannas, A. M., Jones, A. E., Dibb, J., Ammann, M., Anastasio, C., Beine, H. J., Bergin, M., Bottenheim, J., Boxe, C. S., Carver, G., Chen, G., Crawford, J. H., Domine, F., Frey, M. M., Guzman, M. I., Heard, D. E., Helmig, D., Hoffmann, M. R., Honrath, R. E., Huey, L. G., Hutterli, M., Jacobi, H. W., Klan, P., Lefer, B., McConnell, J., Plane, J., Sander, R., Savarino, J., Shepson, P. B., Simpson, W. R., Sodeau, J. R., von Glasow, R., Weller, R., Wolff, E. W., and Zhu, T.: An overview of snow photochemistry: evidence, mechanisms and impacts, Atmos. Chem. Phys., 7, 4329–4373, doi:10.5194/acp-7-4329-2007, 2007.
Hoffer, A., Gelencsér, A., Guyon, P., Kiss, G., Schmid, O., Frank, G. P., Artaxo, P., and Andreae, M. O.: Optical properties of humic-like substances (HULIS) in biomass-burning aerosols, Atmos. Chem. Phys., 6, 3563–3570, doi:10.5194/acp-6-3563-2006, 2006.
Honrath, R. E., Lu, Y., Peterson, M. C., Dibb, J. E., Arsenault, M. A., Cullen, N. J., and Steffen, K.: Vertical fluxes of NOx, HONO, and HNO_3 above the snowpack at Summit, Greenland, Atmos. Environ., 36, 2629–2640, 2002.
Jones, A. E., Weller, R., Anderson, P. S., Jacobi, H. W., Wolff, E. W., Schrems, O., and Miller, H.: Measurements of NOx emissions from the Antarctic snowpack, Geophys. Res. Lett., 28, 1499–1502, 2001.
Jouzel, J., Masson-Delmotte, V., Cattani, O., Dreyfus, G., Falourd, S., Hoffmann, G., Minster, B., Nouet, J., Barnola, J. M., Chappellaz, J., Fischer, H., Gallet, J. C., Johnsen, S., Leuenberger, M., Loulergue, L., Luethi, D., Oerter, H., Parrenin, F., Raisbeck, G., Raynaud, D., Schilt, A., Schwander, J., Selmo, E., Souchez, R., Spahni, R., Stauffer, B., Steffensen, J. P., Stenni, B., Stocker, T. F., Tison, J. L., Werner, M., and Wolff, E. W.: Orbital and millennial Antarctic climate variability over the past 800,000 years, Science, 317, 793–796, doi:10.1126/science.1141038, 2007.
King, M. D., and Simpson, W. R.: Extinction of UV radiation in Arctic snow at Alert, Canada (82° N), J. Geophys. Res.-Atmos., 106, 12499–12507, 2001.
King, M. D., France, J. L., Fisher, F. N., and Beine, H. J.: Measurement and modelling of UV radiation penetration and photolysis rates of nitrate and hydrogen peroxide in Antarctic sea ice: An estimate of the production rate of hydroxyl radicals in first-year sea ice, J. Photochem. Photobiol.y A-Chem., 176, 39–49, 2005.
Lee-Taylor, J. and Madronich, S.: Calculation of actinic fluxes with a coupled atmosphere-snow radiative transfer model, J. Geophys. Res.-Atmos., 107, 4796, doi:10.1029/2002JD002084, 2002.

ACPD
11, 11959–11993, 2011

Legrand, M., Preunkert, S., Jourdain, B., Gallée, H., Goutail, F., Weller, R., and Savarino, J.: Year-round record of surface ozone at coastal (Dumont d'Urville) and inland (Concordia) sites in East Antarctica, J. Geophys. Res., 114, D20306, doi:10.1029/2008jd011667, 2009.
McPeters, R. D., Krueger, A. J., Bhartia, P. K., and Herman, J. R.: Earth Probe Total Ozone Mapping Spectrometer (TOMS) Data Products User's Guide, NASA Reference Publication, 1998.
Neff, W., Helmig, D., Grachev, A., and Davis, D.: A study of boundary layer behavior associated with high NO concentrations at the South Pole using a minisodar, tethered balloons and sonic anemometer, Atmos. Environ., 42, 2762–2779, doi:10.1016/j.atmosenv.2007.01.033, 2008.
Oltmans, S. J., Johnson, B. J., and Helmig, D.: Episodes of high surface-ozone amounts at South Pole during summer and their impact on the long-term surface-ozone variation, Atmos. Environ., 42, 2804–2816, doi:10.1016/j.atmosenv.2007.01.020, 2008.
Oncley, S. P., Buhr, M., Lenschow, D. H., Davis, D., and Semmer, S. R.: Observations of summertime NO fluxes and boundary-layer height at the South Pole during ISCAT 2000 using scalar similarity, Atmos. Environ., 38, 5389–5398, 2004.
Phillips, G. J. and Simpson, W. R.: Verification of snowpack radiation transfer models using actinometry, J. Geophys. Res.-Atmos., 110, D08306, 2005.
Rothlisberger, R., Hutterli, M. A., Sommer, S., Wolff, E. W., and Mulvaney, R.: Factors controlling nitrate in ice cores: Evidence from the Dome C deep ice core, J. Geophys. Res.-Atmos., 105, 20565–20572, 2000.
Rothlisberger, R., Hutterli, M. A., Wolff, E. W., Mulvaney, R., Fischer, H., Bigler, M., Goto-Azuma, K., Hansson, M. E., Ruth, U., Siggaard-Andersen, M. L., and Steffensen, J. P.: Nitrate in Greenland and Antarctic ice cores: a detailed description of post-depositional processes, Ann. Glaciol., 35, 209–216, 2002.
Stamnes, K., Tsay, S. C., Wiscombe, W., and Jayaweera, K.: Numerically Stable Algorithm for Discrete-Ordinate-Method Radiative-Transfer in Multiple-Scattering and Emitting Layered Media, Appl. Optics, 27, 2502–2509, 1988.
Wagenbach, D., Graf, W., Minikin, A., Trefzer, U., Kipfstuhl, J., Oerter, H., and Blindow, N.: Reconnaissance of chemical and isotopic firn properties on top of Berkner Island, Antarctica, Ann. Glaciol., 20, 307–312, 1994.
Wang, Y. H., Choi, Y., Zeng, T., Davis, D., Buhr, M., Huey, L. G., and Neff, W.: Assessing the photochemical impact of snow NOx emissions over Antarctica during ANTCI 2003, Atmos.

ACPD
11, 11959–11993, 2011

Environ., 41, 3944–3958, doi:10.1016/j.atmosenv.2007.01.056, 2007.
Warneck, P. and Wurzinger, C.: Product quantum yields for the 305-nm photodecomposition of nitrate in aqueous solution, J. Phys. Chem., 92, 6278–6283, doi:10.1021/j100333a022, 1988.
Warren, S. G.: Optical-Properties of Snow, Rev. Geophys., 20, 67–89, 1982.
Warren, S. G. and Brandt, R. E.: Optical constants of ice from the ultraviolet to the microwave: A revised compilation, J. Geophys. Res., 113, D14220, doi:10.1029/2007jd009744, 2008.
Warren, S. G., Brandt, R. E., and Grenfell, T. C.: Visible and near-ultraviolet absorption spectrum of ice from transmission of solar radiation into snow, Appl. Optics, 45, 5320–5334, 2006.
Wolff, E. W., Jones, A. E., Martin, T. J., and Grenfell, T. C.: Modelling photochemical NO_x production and nitrate loss in the upper snowpack of Antarctica, Geophys. Res. Lett., 29, 1944, doi:10.1029/2002GL015823, 2002.
Wolff, E. W., Barbante, C., Becagli, S., Bigler, M., Boutron, C. F., Castellano, E., de Angelis, M., Federer, U., Fischer, H., Fundel, F., Hansson, M., Hutterli, M., Jonsell, U., Karlin, T., Kaufmann, P., Lambert, F., Littot, G. C., Mulvaney, R., Rothlisberger, R., Ruth, U., Severi, M., Siggaard-Andersen, M. L., Sime, L. C., Steffensen, J. P., Stocker, T. F., Traversi, R., Twarloh, B., Udisti, R., Wagenbach, D., and Wegner, A.: Changes in environment over the last 800,000 years from chemical analysis of the EPICA Dome C ice core, Quat. Sci. Rev., 29, 285–295, doi:10.1016/j.quascirev.2009.06.013, 2010.
Zellner, R., Exner, M., and Herrmann, H.: Absolute OH quantum yields in the laser photolysis of nitrate, nitrite and dissolved H_2O_2 at 308 and 351 nm in the temperature range 278–353 K, J. Atmos. Chem., 10, 411–425, doi:10.1007/bf00115783, 1990.
Zhu, C., Xiang, B., Chu, L. T., and Zhu, L.: 308 nm Photolysis of Nitric Acid in the Gas Phase, on Aluminum Surfaces, and on Ice Films, J. Phys. Chem. A, 114, 2561–2568, doi:10.1021/jp909867a, 2010.

ACPD
11, 11959–11993, 2011

Table 1. Snowpack properties for each snowpack layer at Dome C.

Snow/ Description	σ_{scatt}/ $m^2\ kg^{-1}$ (350 nm)	σ^+_{abs}/ $cm^2\ kg^{-1}$ (350 nm)	snow T / °C	density / $g\ cm^{-3}$	Snowpack layer thickness/cm	Range of grain size /mm
Soft windpack	14–22 (20)	1.3–2.2 (1.7)	23	0.3	11	0.3–1
Hard windpack	17–24 (19)	1.3–1.8 (1.7)	27	0.38	21	0.3–2
Hoar like layer	8–16 (10)	0.6–1.4 (1.2)	30	0.28	68	1–4

ACPD
11, 11959–11993, 2011

Table 2. Comparison of optical coefficients for Dome C snow layers with previously investigated sites, all optical co-efficient measurements are for a wavelength of 400 nm.

Study	Snow description	Measurements?		γ_{matt}	γ_{abs}	
		e-fold	reflectivity	$m^2\ kg^{-1}$	$cm^2\ kg^{-1}$	notes
Grenfell and Maykut (1977)	Arctic Summer dry	✓	✓	6.4	7.3	
	Arctic summer melting	✓	✓	1.1	7.8	
Grenfell et al., 1994)	Antarctic South Pole	✓	✓	6–25	0	
King and Simpson (2001)	Arctic spring windblown	✓	x	6–30	4–5	
Beaglehole et al. (1998)	Antarctic summer coastal	✓	x	7–13	0.4	snow not measured in situ
Fisher et al. (2005)	Mid-latitude windslab - melting	✓	✓	1	1	
	Mid-latitude windslab - dry	✓	✓	2–5	1–2	
Beine et al. (2006)	Antarctic coastal hard windpack	✓	✓	1.3	4.3	
	Antarctic coastal soft windpack	✓	✓	6.3	24	
	Antarctic coastal recent windblown	✓	✓	3.7	37	
	Antarctic coastal precipitation	✓	✓	4.3	17	
France et al. (2011)	Fresh Ny-Ålesund snowpack	✓	✓	16.7	2.7	
	Melting Ny-Ålesund snowpack	✓	✓	0.8	19.8	
France et al. (2011)	Ny-Ålesund – old windpack	✓	✓	9.5	1.4	
	Ny-Ålesund – fresh windpack	✓	✓	7.7	5.3	
	Ny-Ålesund – marine influenced	✓	✓	20	3.4	
	Ny-Ålesund – glacial	✓	✓	25.5	0.5	
This Work	Dome C – soft windpack	✓	✓	20–42	0.5–1.1	
	Dome C – hard windpack	✓	✓	18–40	0.2–1.4	
	Dome C – hoar like layer	✓	✓	9–18	0.5–1.8	

ACPD
11, 11959–11993, 2011

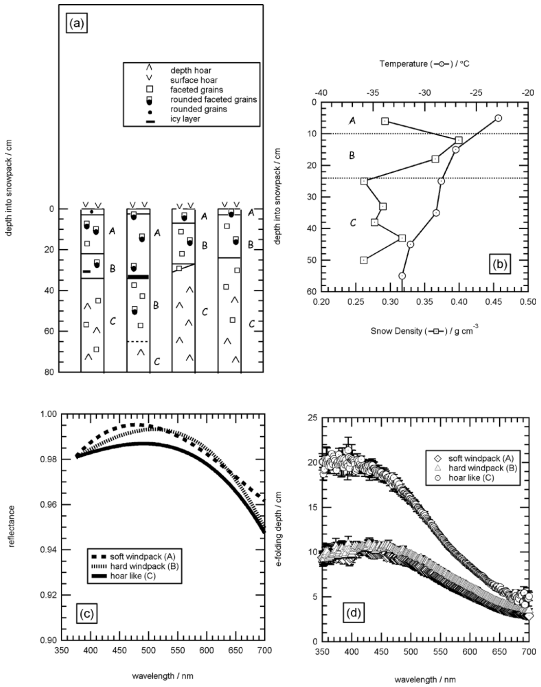

Fig. 1. **(a)** Snowpack stratigraphy measurements from four snowpacks at / near Dome C between 19 December 2009 and 13 January 2010 to demonstrate the uniformity of the snowpack in the area, symbols used from the International classification of snow on the ground (Fierz et al., 2009). Layers are summarised into A, B and C as referred to in the text and tables in the rest of the paper as soft windpack (A), hard windpack (B) and hoar-like (C). The average snowpack stratigraphy as measured is shown in Table 1. **(b)** Measured snowpack temperature and density profiles across the snow layers from the snowpack measured on 6 January 2010, a typical snowpack stratigraphy for the sampled region. Temperatures measured at local noon. **(c)** Nadir reflectivity versus wavelength measured for each of the snowpack layers corresponding to the *e*-fold measurements in Fig. 1d, 2 standard deviation errors are typically 1.5 from the mean and are omitted for clarity. **(d)** Comparison of median average *e*-folding depths versus wavelength for each of the snowpack layers, error bars are 2 standard deviation from the mean value. The median is plotted to demonstrate the set of measured set of results (e-fold and albedo from the same location) used to determine optical coefficients rather than a composite of measurements.

ACPD
11, 11959–11993, 2011

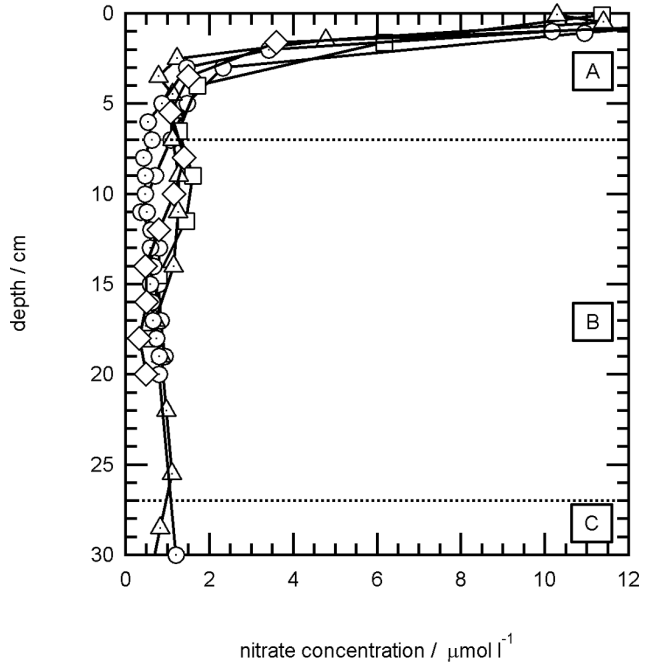

Fig. 2. Measured snowpack nitrate concentrations at Dome C from two sites during December 2009 to Jan 2010. Dashed lines are the stratigraphy changes within a typical snowpack profile demonstrating the uniformity of nitrate profile within the snow cover at Dome C. The dotted circles represent the nitrate profile used in the calculation of NO_2 flux measurements as it was measured at the site of the majority of snowpack *e*-fold and reflectivity measurements.

ACPD
11, 11959–11993, 2011

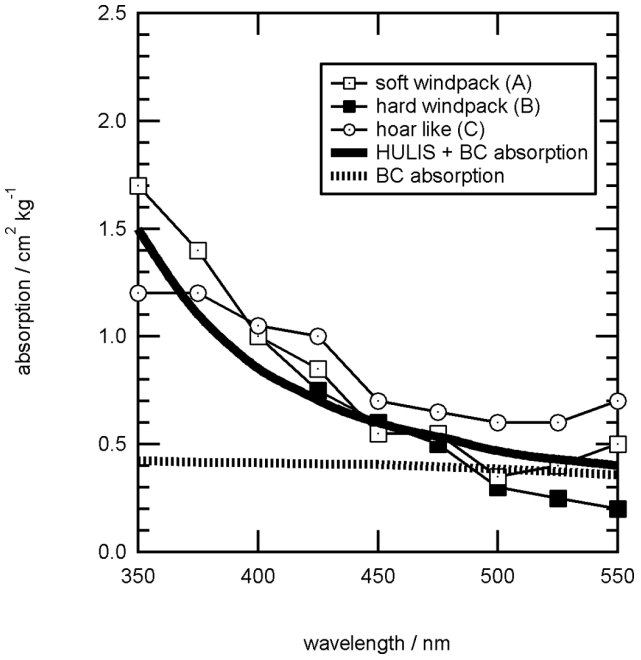

Fig. 3. Total absorption due to impurities cross-section for each Dome C snowpack layer. The absorption cross-section is expected to be a combination of absorbers such as black carbon, mineral dust and humic material/HULIS. The absorption is scaled in terms of black carbon equivalence. Overprinted in dashed line is an absorption due to only black carbon. To give an absorbance cross-section to mimic the absorption seen in the total snowpack absorption due to impurities the solid black line is an absorption due to a mixture of black carbon and HULIS (Hoffer et al., 2006).

ACPD
11, 11959–11993, 2011

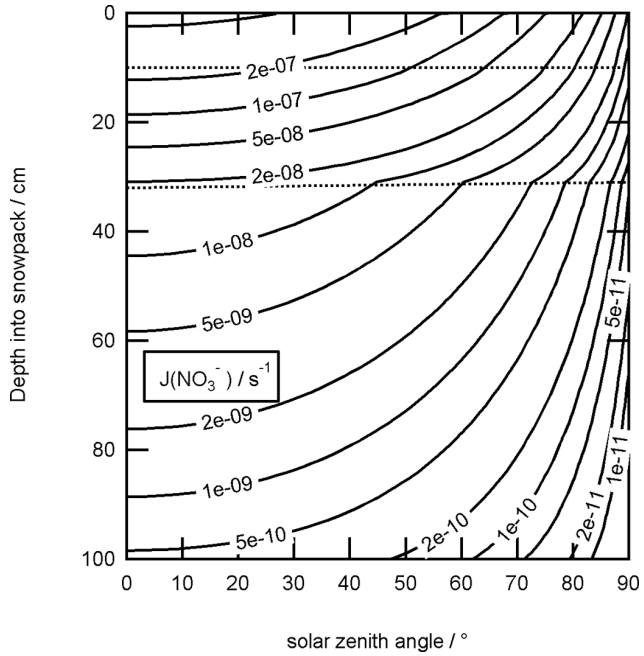

Fig. 4. Nitrate photolysis rate co-efficient contours for a Dome C snowpack stratigraphy, (as described in Table 1), plotted against solar zenith angle and depth into the snowpack. Horizontal dashed lines represent the changes in the snowpack stratigraphy.

ACPD
11, 11959–11993, 2011

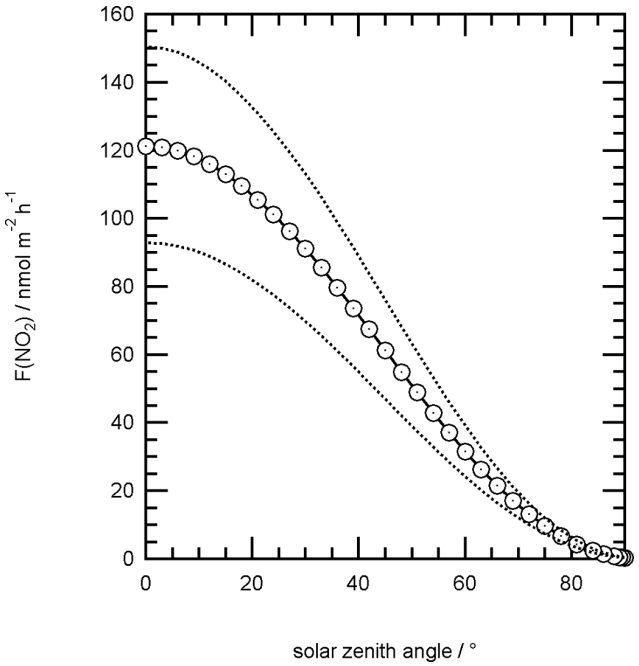

Fig. 5. Maximum flux of NO_2 from the snowpack versus solar zenith angle, assuming all photoproduced NO_2 from nitrate photolysis is liberated to the atmosphere. The snowpack stratigraphy is taken from Table 1. The central line (dotted circles) is calculated using the dotted circled nitrate profile from Figure 2. The dotted lines above and below represent minimum and maximum NO_2 fluxes calculated using the other measured nitrate profiles shown in Fig. 2.

ACPD
11, 11959–11993, 2011

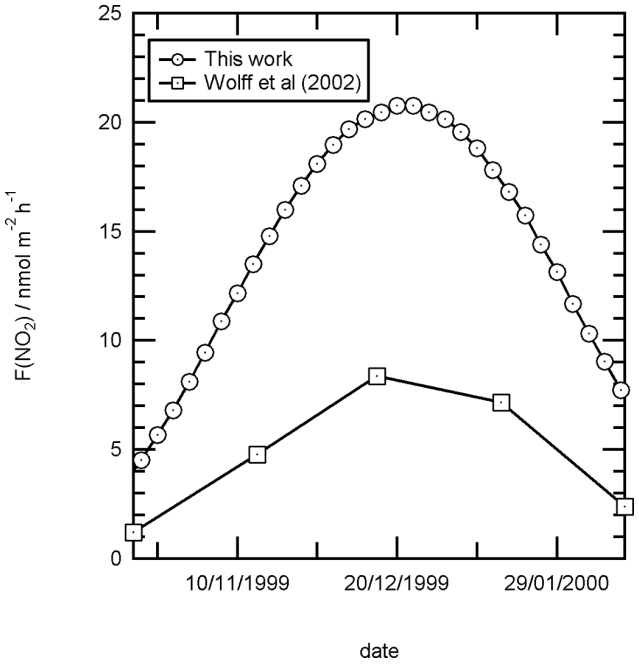

Fig. 6. Modelled fluxes of NO_2 from a South Pole site assuming the snowpack properties are the same as Dome C as a direct comparison with the work of Wolff et al. (2002). The central line (dotted circles) is calculated using the dotted circled nitrate profile from Fig, 2. The dotted lines above and below represent minimum and maximum NO_2 fluxes calculated using the other measured nitrate profiles shown in Fig. 2.

ACPD
11, 11959–11993, 2011

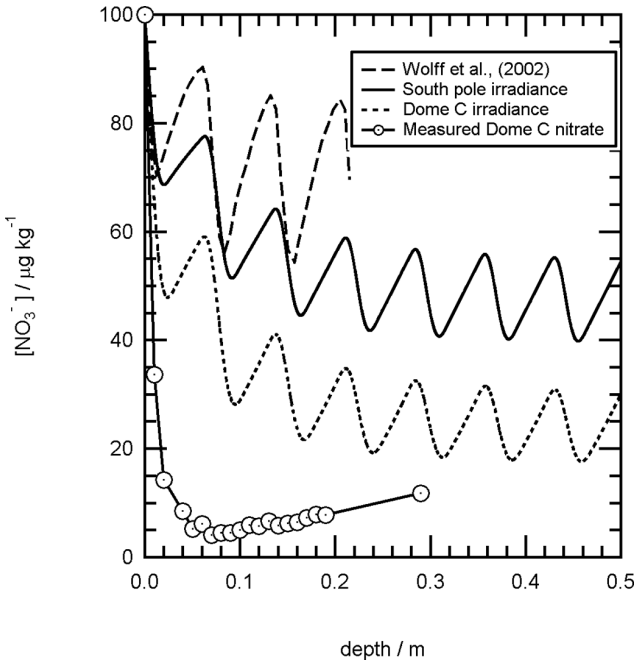

Fig. 7. Depletion of nitrate concentration with depth into the snowpack due to only photochemistry, assuming clear sky South Pole irradiance and clear sky Dome C irradiance, a Dome C accumulation rate (6 mm per month) and a deposited nitrate concentration of 100 µg kg^{-1} continuously deposited year round. The nitrate concentration profile measured within the snowpack at Dome C was measured on 11 January 2010 and has been scaled to 100 µg kg^{-1} at the surface.

ACPD
11, 11959–11993, 2011